	Experiment title: Application of the synchrotron radiation based high-resolution GEXRF for studies of periodic surface nanostructures	Experiment number: MI-1108
Beamline: ID21	Date of experiment: from: 23 Nov 2012 to: 29 Nov 2012	Date of report: 22.11.2011
Shifts: 18	Local contact(s): Murielle Salome	*Received at ESRF: 26.11.2012*

Names and affiliations of applicants (* indicates experimentalists):

S. H. Nowak*, Département de Physique, Université de Fribourg, CH-1700 Fribourg, Suisse
D. Banaś*, Institute of Physics, Jan Kochanowski University, 25-406 Kielce, Poland
W. Błachucki*, Département de Physique, Université de Fribourg, CH-1700 Fribourg, Suisse
J.-Cl. Dousse*, Département de Physique, Université de Fribourg, CH-1700 Fribourg, Suisse
P. Hoenicke*, Physikalisch-Technische Bundesanstalt, 10587 Berlin, Germany
J. Hoszowska*, Département de Physique, Université de Fribourg, CH-1700 Fribourg, Suisse
Y. Kayser*, Département de Physique, Université de Fribourg, CH-1700 Fribourg, Suisse
A. Kubala-Kukuś*, Institute of Physics, Jan Kochanowski University, 25-406 Kielce, Poland
M. Pajek*, Institute of Physics, Jan Kochanowski University, 25-406 Kielce, Poland
F. Reinhardt*, Physikalisch-Technische Bundesanstalt, 10587 Berlin, Germany
J. Szlachetko*, Institute of Physics, Jan Kochanowski University, 25-406 Kielce, Poland

Report:

Introduction

The purpose of the present experiment was to check the utility of the synchrotron radiation based high-resolution Grazing Emission X-Ray Fluorescence (GEXRF) technique [1] for the surface characterization of samples consisting of metallic periodic structures deposited on silicon substrates. TXRF (Total reflection X-Ray Fluorescence) and GEXRF are well known for their utility in surface analysis [2]. Similarly to TXRF, the GEXRF method serves as a very sensitive tool for trace element analysis, thin layer characterization, and non-destructive depth profiling.

The operational principle of the GEXRF technique [3,4] consists in measuring the intensity evolution of a fluorescence x-ray line around its critical angle of total reflection φ_c. It can be regarded as a time-reversed TXRF experiment [2]. For exit angles below φ_c, due to the evanescent wave propagation, only the first few nanometers in the depth direction contribute to the measured intensity. For exit angles larger than φ_c, the detection setup becomes sensitive to x-rays emitted deeper inside the sample. In this angular range the accessible depth region is limited by the self-absorption of the fluorescence x-rays.

Depending on the sample morphology three well described types of GEXRF angular profiles are observed, namely bulk-like, layer-like and particle-like profiles [3,4]. For bulk-like structures the emitted radiation is refracted once at the vacuum-bulk interface and the evolution of the GEXRF angular profile follows approximately the variation of the transmission coefficient. For layer-like structures, at angles above φ_c, many reflections occur leading to the observation of interference patterns in the detected fluorescence. For particle-like structures the angular profile results from the sum of the direct and singly reflected radiation. Thereby, below φ_c the x-ray intensity is twice that of the substrate.

Furthermore, according to simulations performed using a numerical model based on Geometrical Optics (GO), it was expecting the GEXRF angular profiles of surfaces with periodic structures to exhibit additional interference patterns from which a detailed information about the distribution and dimensions of the structure components could be then deduced.

Experiment

The experiment was performed at the ESRF beam line ID21 using the high-resolution von Hamos Bragg-type bent crystal spectrometer of Fribourg [5] for the detection of the sample x-ray fluorescence. For all measurements the von Hamos spectrometer was equipped with a SiO_2 (1-10) crystal. The beam line setup consisted of two undulators mounted in series, a Ni coated mirror for the upper harmonics rejection and a NiB4C multilayer monochromator. The beam energy was tuned to 6.48 keV. Two slits with adjustable widths and perpendicular to each other were used to define the beam size. The latter varied between 0.05×0.2 mm^2 and 1.2×1.2 mm^2. For the biggest beam size, the intensity on the sample was $2.8 \cdot 10^{13}$ photons/s. During the experiment the GEXRF angular profiles of Cr nanostructures with different periodic patterns (stripes, trapezoidal prisms, disks) deposited on Si wafers were measured using the Kα x-ray fluorescence lines of Cr and Si, the Si Kα x-ray line being observed in first order of diffraction, the Kα x-ray line of Cr in second order.

Results

Cr Stripes

The sample was prepared by means of the lift-off technique using a Si wafer having a native oxide layer of ~3 nm. A pattern of 1000 stripes having a length of 6 mm and a width of 1 µm distributed with a period p_0 = 6 µm was imprinted on the photoresist. The latter was then covered with a thin chromium layer. After removal of the photoresist 10 nm high Cr stripes remained on the sample surface.

The Cr stripes sample was measured at different angles ϑ by rotating it around an axis perpendicular to its surface. This allowed us to investigate the GEXRF profiles of the structure for different periods $p=p_0/\sin\vartheta$.

For $\vartheta = 0$ the GEXRF spectrum exhibits a layer-like profile similar to the one corresponding to a Cr layer having a thickness of 10 nm, i.e., the nominal thickness of the structure. When increasing ϑ, a characteristic peak as the one observed in particle-like profiles becomes visible at the critical angle for total reflection in Si (φ_{Si}). When recording the GEXRF spectra at still larger values of ϑ, intensity modulations can be observed above φ_{Si}. The frequency of the modulation which decreases with the sine of the rotation angle ϑ can be calculated from the refractive index n_{Cr}, height h, and period p of the Cr structure using the above mentioned GO model.

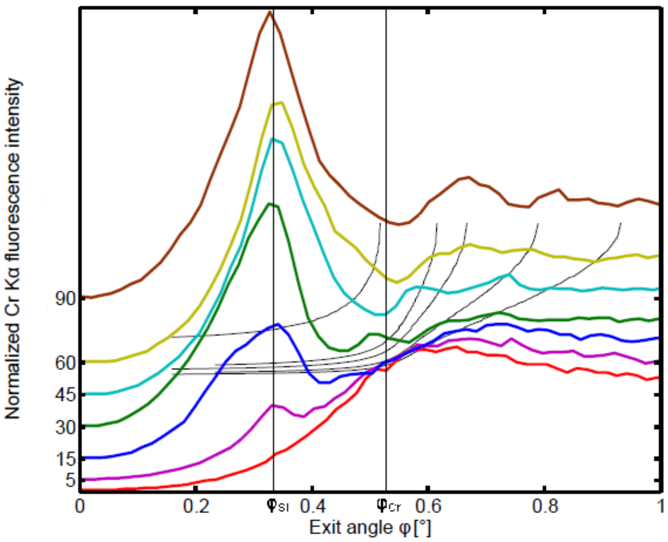

Figure 1: GEXRF profiles of the Cr stripes sample for different orientations ϑ of the latter. The grey curves indicate the positions of the intensity modulation maxima predicted by the calculations. The two black vertical lines represent the critical angles for total reflection in Si (substrate) and Cr (periodic structure). To better separate the curves corresponding to different sample orientations, intensity offsets equal to the values of ϑ were used.

Trapezoidal prisms

A 10 cm in-diameter Si (110) wafer was used as substrate. The latter was first cleaned with a O_2 plasma and a Piranha solvent. A 10.7 nm thick chromium layer was then deposited on the wafer by means of thermal evaporation at room temperature. The layer was then coated with a photoresist and the pattern of juxtaposed trapezoidal prisms was imprinted by a PC-controlled high-resolution laser beam. The pattern consisted of identical trapezoidal prisms having a length of 2 mm and widths varying from 2 µm to 10 µm; the distance between the prims was p = 12 µm. After development of the photoresist a wet etched Cr layer was obtained. Finally, the remaining photoresist was removed.

All the measurements were performed for the same sample surface orientation, namely the one for which the detected radiation propagated across the trapezoidal prisms. The spectra were observed for various positions of the beam spot on the structure in order to investigate the variation of the GEXRF profiles as a function of the prism width while keeping the structure period p fixed.

The results demonstrate a strong dependence of the GEXRF profiles on the prism width. The most visible changes concern the angular region lying between φ_{Si} (the critical angle of the substrate) and φ_{Cr} (the critical angle of the structure material). At φ_{Si} a peak is observed which is characteristic for particle-like profiles. Around φ_{Cr} the intensity increases again so that a minimum of intensity is observed between the two critical angles. The depth of this intensity valley decreases with the prism width. For wide prisms the particle-like peak is no more visible but the GEXRF intensity below φ_{Cr} is still enhanced with respect to that of the

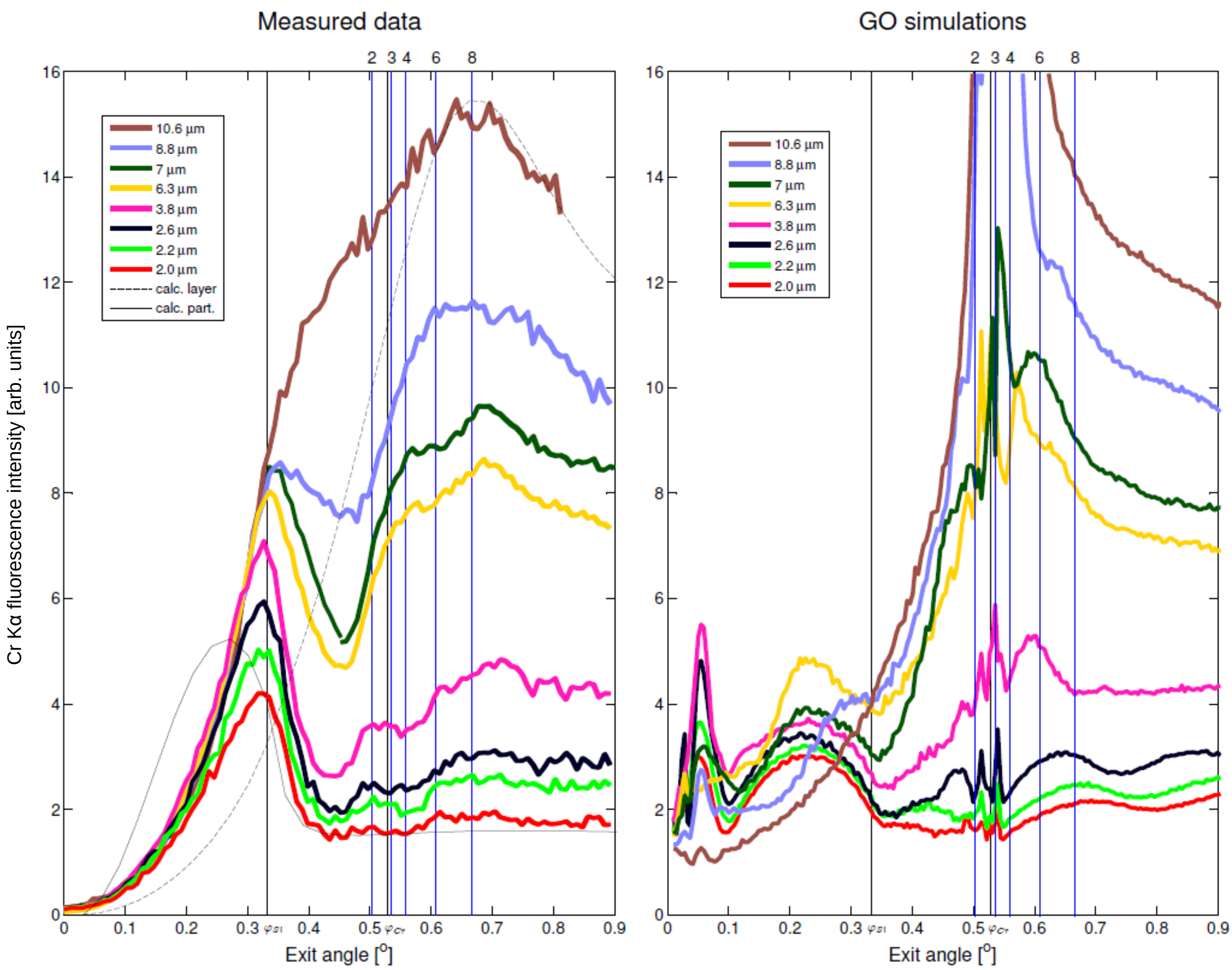

Figure 2: Experimental GEXRF profiles of the sample with Cr trapezoidal prisms (left panel) and results of GO calculations performed using a rms roughness of 1 nm (right panel). The fluorescence intensities are normalised and scaled to the prism widths. Dashed grey line: calculated profile of a 10.7 nm Cr layer scaled to the intensity of a 10.6 µm wide prism. Solid grey line: calculated profile of a 10.7 nm Cr particle scaled to the intensity of a 2 µm wide prism. Vertical lines: blue – calculated intensity modulation positions; black – critical angles for Si and Cr.

calculated layer-like profile. Effects of multiple reflections can also be seen.

In Figure 2 the experimental results and performed GO calculations are compared. Even though the GO simulations do not reproduce precisely the measured data the main trends are correctly represented. We can indeed observe a very similar evolution of the intensity valley between the critical angles φ_{Si} and φ_{Cr}. The modulation of the intensity due to multiple reflections is also similar.

However, the sharp peak around 0.5° is a digital artifact which has no physical meaning. Also, for wider prisms, the simulations most significantly differ from the measurements around φ_{Cr}. This difference can be attributed to the limited optical paths coherence that has not been considered in the present simulations.

Conclusions

As predicted by the GO based model characteristic interference patterns are visible for the GEXRF profiles of periodic structures. We believe that systematic GO simulations can significantly contribute to the development of more precise TXRF quantification models for particulate media. Such a new quantification method would be especially useful for densely packed nanodevices or nanoparticles sampled directly from the aerosol phase and from dried liquid droplets.

References

[1] J. Szlachetko, D. Banaś, A. Kubala-Kukuś, M. Pajek, W. Cao, J.-Cl. Dousse, J. Hoszowska, Y. Kayser, M. Szlachetko, M. Kavčič, M. Salomé, and J. Susini, “Application of the high-resolution grazing-emission x-ray fluorescence method for impurities control in semiconductor nanotechnology,” *J. Appl. Phys.*, vol. 105, p. 086101, 2009.

[2] K. Stoev and K. Sakurai, “Review on grazing incidence X-ray spectrometry and reflectometry,” *Spectrochim. Acta, Part B*, vol. 54, no. 1, pp. 41–82, 1999.

[3] D. K. G. de Boer, “Glancing-incidence x-ray fluorescence of layered materials,” *Phys. Rev. B*, vol. 44, pp. 498–511, 1991.

[4] H. P. Urbach and P. K. de Bokx, “Calculation of intensities in grazing-emission x-ray fluorescence,” *Phys. Rev. B*, vol. 53, no. 7, pp. 3752–3763, 1996.

[5] J. Hoszowska, J.-Cl. Dousse, J. Kern, and C. Rhême, “High-resolution von Hamos crystal X-ray spectrometer,” *Nucl. Instrum. Methods Phys. Res., Sect. A*, vol. 376, no. 1, pp. 129–138, 1996.